Research on effects of active fiber length and dopant concentration on 976-nm Yb-doped fiber amplifiers

Ruixing Wang (王睿星), Jianqiu Cao (曹涧秋)*, Ying Liu (刘 莹), Shaofeng Guo (郭少锋), and Jinbao Chen (陈金宝)

College of Opto-Electronic Science and Engineering, National University of Defense Technology, Changsha 410073, China

**Corresponding author: jq_cao@126.com*

Received January 30, 2013; accepted March 10, 2013; posted online July 17, 2013

In this letter, the theoretical model and rate equations of Ytterbium-doped double-clad fiber amplifiers are introduced. The output performance of fiber amplifiers is analyzed through numerical simulations considering three main factors: active fiber length, pump power, and dopant concentration. It is found that the output signal power experiences a stable growth and then decreases rapidly as the active fiber length becomes longer. It is also revealed that the dopant concentration shows similar effects as active fiber length on the output signal power of fiber amplifiers.

OCIS codes: 060.2320, 140.3615, 140.4480, 060.2280.

doi: 10.3788/COL201311.S20603.

The output power of fiber lasers with high beam quality has been increasing rapidly in the last decade from several watts in 2003 to 10 kW in 2010[1], owing to the invention and development of Ytterbium-doped double-clad fiber. Yb-doped fiber laser (YDFL) is the focus of the field of lasers in recent years because of its excellent properties such as high output power, high efficiency, excellent beam quality, and its compactness. An absorption peak of Yb-ion at the wavelength around 976 nm makes it excellent pump source for high power lasers. However, most of the high power fiber lasers use the 980-nm laser diode (LD) as the pump source, whose low beam quality limits the further exploration of YDFL. An alternative of high quality 976-nm fiber lasers may solve the problem as both high power and high quality pump source.

The approximately equal absorption and emission cross-section[2] of Yb-ions near 976 nm makes it more difficult to generate radiation near 976-nm wavelength than the unwanted amplified spontaneous emission (ASE) with the peak at 1 030 nm in 976-nm lasers or amplifiers. To suppress the ASE and to overcome the re-absorption at 976 nm, a relative high population inversion of about 50% is required. An essential way of reducing the ASE is to enlarge the ratio of core area to effective mode field area[3]. In 2002, Kurkov *et al.* reported the maximum output power of 1.2 W at 978 nm for a launched pump power of 3.8 W[4]. Later, 977-nm fiber lasers of multi-watt level of radiation were claimed successful by the use of ring-doped and jacketed-air-clad (JAC) Yb-doped fiber in Southampton[5,6]. In 2008, 94-W output power at 976 nm with excellent beam quality has been demonstrated by Roser *et al.* by using a rod-type photonic crystal fiber (PCF) which provides a large mode area while maintaining the high beam quality[7]. In the same year, Boullet *et al.* using the PCF with the same properties got similar results[8]. More recently, in 2011 Bartolacci, *et al.* used the standard single-mode Yb-doped fiber as the active fiber for 980-nm amplification of a master oscillator power amplifer (MOPA) scheme[9].

Most of the state-of-the-art high-powered fiber lasers involve the MOPA schemes, which consist of a low power master oscillator and followed by a high power fiber amplifier. The high power fiber amplifier plays a significant role in high power lasers. However, very limited studies were carried out on the properties of the 976-nm Yb-doped fiber amplifiers. In this letter, the output properties of continuous wave fiber amplifiers are discussed and several suggested value of parameters is given.

A schematic representation of the structure of the forward-pumped fiber amplifier is depicted in Fig. 1. Unlike the fiber lasers which have cavity reflectors, the fiber amplifier has three main components: laser source, pump source, and gain fiber. The cleaved angle at the end of the amplifier is used to suppress the reflection of the ASE around 1 030 nm.

The operation of the amplifier, especially in the doped fiber, can be modeled by a set of rate equations[10]. In this mathematical model the excited state absorption (ESA) has been ignored because the procedure of non-radioactive transition is very fast. The rate equations of the stead-state are as

$$\frac{N_2(z)}{N}=\frac{\frac{\left[P_{\rm p}^{+}(z)+P_{\rm p}^{-}(z)\right]\Gamma_{\rm p}\sigma_{\rm ap}}{h\nu_{\rm p}A}+\frac{\Gamma_{\rm s}}{hcA}\int\sigma_{\rm a}(\lambda)\cdot\left[P^{+}(z,\lambda)+P^{-}(z,\lambda)\right]\lambda{\rm d}\lambda}{\frac{\left[P_{\rm p}^{+}(z)+P_{\rm p}^{-}(z)\right](\sigma_{\rm ap}+\sigma_{\rm ep})\Gamma_{\rm p}}{h\nu_{\rm p}A}+\frac{1}{\tau}+\frac{\Gamma_{\rm s}}{hcA}\int\left(\sigma_{\rm a}(\lambda)+\sigma_{\rm e}(\lambda)\right)\cdot\left[P^{+}(z,\lambda)+P^{-}(z,\lambda)\right]\lambda{\rm d}\lambda},\tag{1}$$

$$\pm\frac{{\rm d}P^{\pm}(z,\lambda)}{{\rm d}z}=\Gamma_{\rm s}\{\left[\sigma_{\rm e}(\lambda)+\sigma_{\rm a}(\lambda)\right]N_2(z)-\sigma_{\rm a}(\lambda)N\}\cdot P^{\pm}(z,\lambda)+\Gamma_{\rm s}\sigma_{\rm e}(\lambda)N_2(z)P_{\rm o}(\lambda)-\alpha(z,\lambda)P^{\pm}(z,\lambda),\tag{2}$$

$$\pm\frac{{\rm d}P_{\rm p}^{\pm}(z)}{{\rm d}z}=-\Gamma_{\rm p}\{\sigma_{\rm ap}(N-N_2(z))-\sigma_{\rm ep}\}\cdot P_{\rm p}^{\pm}(z)-\alpha(z,\lambda_{\rm p})P_{\rm p}^{\pm}(z),\tag{3}$$

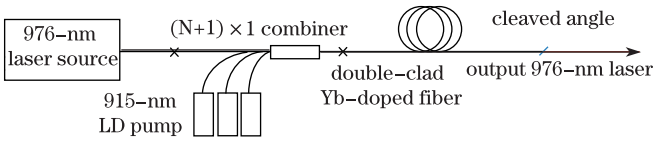

Fig. 1. The scheme of 976-nm fiber amplifier.

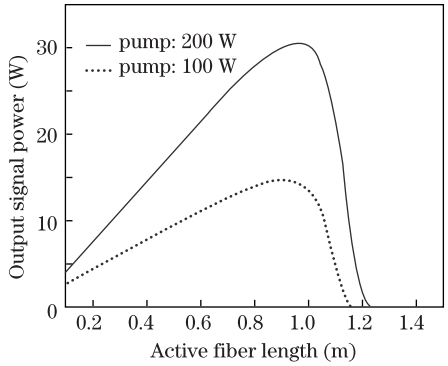

Fig. 2. Output signal powers for different active fiber lengths for pump power are 200 and 100 W, respectively.

where N is the dopant concentration (averaged per unit volume) and $N_2(z)$ is the population density of the excited state. The power of the signal and the ASE are all represented by $P^{\pm}(z, \lambda)$, considering the different the wavelengths. ${P_{\rm p}}^{\pm}(z)$ is the pump power at the wavelength of $\lambda_{\rm p}$. The plus sign and the minus sign are indicated the positive and negative propagation along the z-direction, respectively. The pump power filling factor $\Gamma_{\rm p}$ approximately equals the ratio of core to cladding area while The signal power filling factor is Γs. $\sigma_{\rm e}(\lambda)$ and $\sigma_{\rm a}(\lambda)$ are the wavelength dependent emission and absorption cross section. $\sigma_{\rm ep}$ and $\sigma_{\rm ap}$ are abbreviation of $\sigma_{\rm e}(\lambda_{\rm p})$ and $\sigma_{\rm a}(\lambda_{\rm p})$ at the pump wavelength. $\alpha(z, \lambda)$ is the scattering loss with wavelength dependent. τ is the spontaneous emission lifetime, A is the efficient dopant cross section area, c is the speed of light in vacuum, and h is Planck's constant. The spontaneous emission $P_0(\lambda)$ which results in the initial ASE is given by[11]

$$P_0(\lambda) = 2hc^2/\lambda^3. \tag{4}$$

Our numerical research is based on these equations discussed above. Together with the initial pump power and the signal power, we can get our numerical results.

The effects of several parameters on the performance of forward-pumped fiber amplifiers have been discussed as following. The main parameters involved are length of the active fiber, the pump power, and the dopant concentration. In the simulation, we assume the signal power, concentrates on the wavelength of 976 nm. Unless otherwise stated, parameters used in the simulations are listed in Table 1.

The active fiber length lays a significant role on the performance of fiber amplifiers. Here, we control other parameters and observe the relationship between active fiber length and the output power. Figures 2–4 illustrate the changes of output power (including signal and ASE while excluding the remaining pump power) with various fiber lengths.

Table 1. Parameters Used in Simulationl

Parameter	Value	Parameter	Value
$\lambda_{\rm p}$(nm)	915	$\Gamma_{\rm p}$	0.0133
$\lambda_{\rm s}$(nm)	976	$\Gamma_{\rm s}$	0.95
τ(ms)	0.84	$N(\rm m^{-3})$	3.95×10^{25}
$\sigma_{\rm a}(\lambda)$	See Ref. [2]	Core Diameter(μm)	15
$\sigma_{\rm e}(\lambda)$	See Ref. [2]	Clad Diameter(μm)	130
$\alpha_{\rm p}$	0.0023	Seed Power(W)	1
$\alpha(\lambda)$	0.005		

Figure 2 displays the output signal power when using various active fiber lengths. See from the graph, the output signal power for both pump source experiences a steady increase with the fiber length at first, while when the length reaches about 1 m the signal power gets its maximum value, and then it decreases exponentially to approximate zero at about 1.2 m. The output power spectrum with various active fiber lengths shown in Fig. 3 gives an additional description for this. Figure 3(a) exhibits the output spectrum when the fiber is shorter than the optimum length, and as we can notice, the shorter the length is, the more undesired ASE near 1 030 nm is suppressed. Spectra using longer active fiber are shown in Fig. 3(b), the signal power at 976 nm is diminished as the fiber gets longer, and at last vanishes.

The output power of ASE in 976-nm fiber lasers and amplifiers mainly gathers around 1 030 nm and it increases with the fiber length which is displayed in Fig. 4. The ASE power is barely seen until the fiber is about 0.8 m, and then it experiences a prompt increase exponentially and at last becomes linear ascending.

This relationship can be explained as followed. When the active fiber length is shorter than the optimum length, the inversion of Yb-ions provided by the pump power can meet the condition of 976-nm emission and the ASE around 1 030 nm is relatively low.

As the active fiber length gets longer, just after reaching the optimum length, namely 0.96 m for 200-W pump and 0.91 m for 100-W pump in the simulation, the pump power is not enough to maintain the inversion condition for 980-nm amplification all along the fiber and causes the enhance of 1 030-nm emission. Furthermore, in this period, the re-absorbed 976-nm radiation also serves as high-efficient pump source of the ASE and thus leading to the rapid increase of ASE. After this, the ASE around 1 030 nm which is dominant in fiber amplifiers increases linearly with the fiber length. So the optimization of the active fiber length is important for the suppression of the ASE and the optimization of the amplifier.

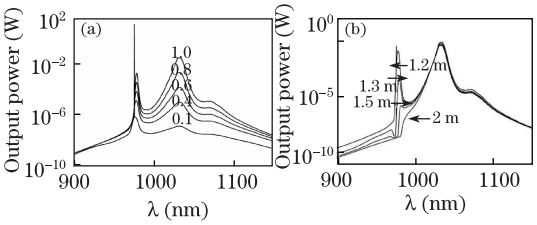

Fig. 3. Spectra of output power using different fiber lengths of (a) 0.1, 0.4, 0.6, 0.8 and 1 m and (b) 1.2, 1.3, 1.5 and 2 m.

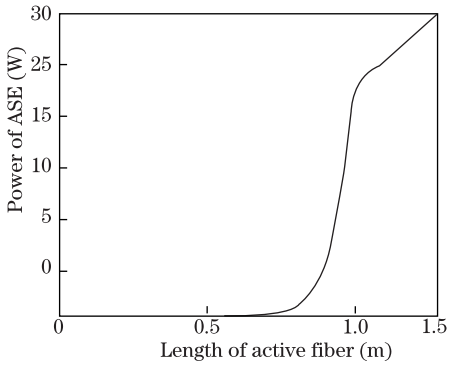

Fig. 4. Output power of ASE versus fiber length.

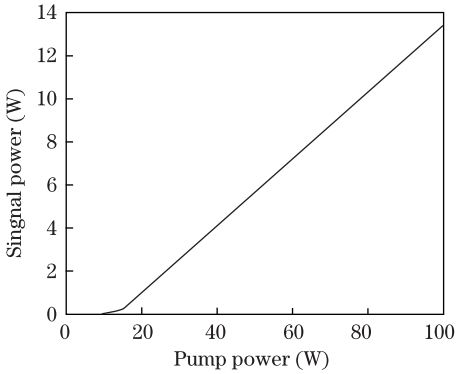

Fig. 5. Output sig nal power versus. pump power.

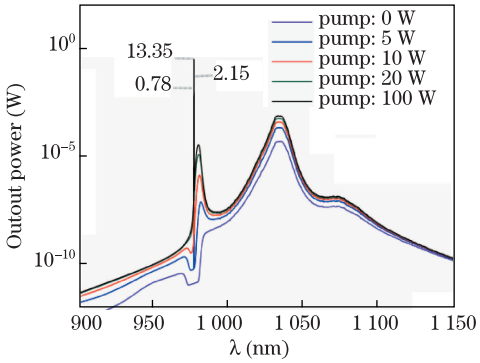

Fig. 6. (Color online) Spectra of output power at different pump powers.

The pump power is a key factor for the assurance of high inversion of Yb-ion population for 976-nm emission and furthermore, to suppress the undesired ASE. Figures 5 and 6 reveal the relationship between output power and the pump power. The initial signal power used for simulation is 1 W and the fiber length is 1 m. The signal laser at 976 nm hardly appears before the pump power gets to specific value, namely the pump threshold, and after that point the signal power rises linearly. When the pump power is lower than its threshold (about 13 W), the ASE power overweighs the signal power due to the low population inversion which promotes 1 030 nm emission as discussed above. As the result, the signal power is hard to generate. When the pump power is just larger than the threshold, the slow increase of signal power indicates the competition of radiation between 976 nm and wavelengths around 1 030 nm. When the pump power is large enough, the signal emission outweighs the ASE and thus resulting in the steady linear ascent of signal power with pump power. In the simulation, the pump efficiency is about 16%.

Here we put the effects of both pump power and active fiber length together. The output signal power and ASE power are shown in Figs. 7 and 8 respectively. We can clearly notice that the trend of signal power and the ASE. It is also found in Fig. 7 that the optimum fiber length is basically stable to various pump power. The contour line of the output signal power and ASE power are shown in Fig. 9. The Line "a" in Fig. 9 which represents the output signal power of 1 W determines the pump threshold-the pump power needed for the amplification of signal power-increasing with the active fiber length. The rapid decrease of signal power in Fig. 7 and the fast increase of ASE power in Fig. 8 can be explained by the competition of gains between 976 nm and wavelengths around 1 030 nm shown in the region of intersection between signal and ASE in Fig. 9.

Subsequently, we investigate the influence of dopant concentration on output performance of fiber amplifiers. Figure 10 exhibits the variation of output signal power in different dopant concentrations. The initial signal power is 1 W and the active fiber length is 0.5 m. The pump powers being used in the simulation are 100 and 200 W, respectively.

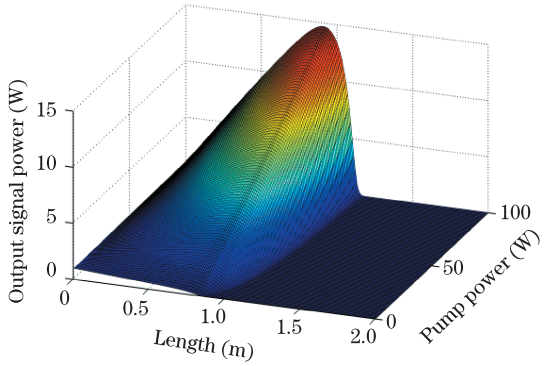

Fig. 7. (Color online) Output signal power versus active fiber length and pump power.

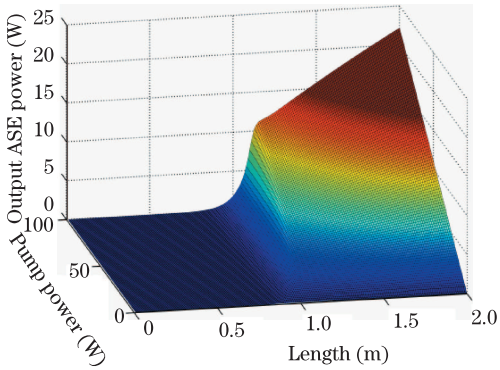

Fig. 8. (Color online) Output ASE power versus active fiber length and pump power.

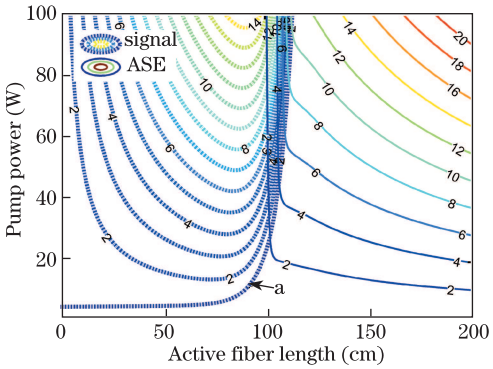

Fig. 9. (Color online) Contour line of output signal and ASE power.

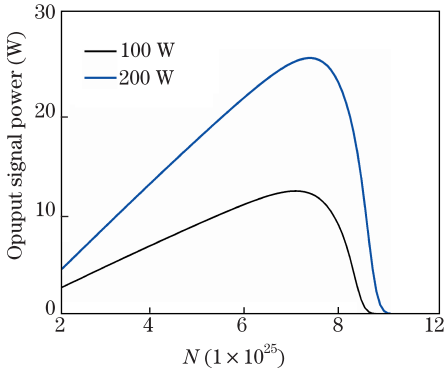

Fig. 10. (Color online) Output signal power versus different dopant concentrations.

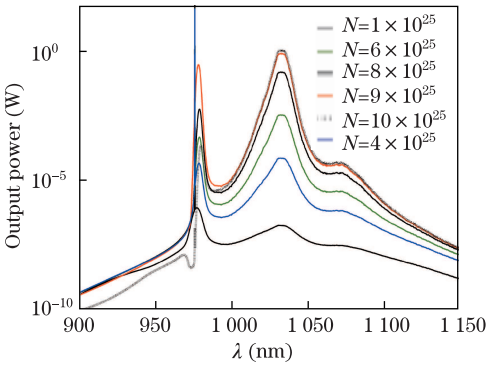

Fig. 11. (Color online) Spectra of output power.

Similar to active fiber length, the signal power increases firstly and after one certain point drops to zero rapidly, which indicates that a relative high dopant concentration needs higher pump power to meet the inversion requirement. However, if the dopant concentration is so high that the pump power cannot meet the inversion requirement, the ASE is dominant in the amplifier, and the signal power at 976 nm will be suppressed and vanish at the output end. The spectrum of the output radiation via various dopant concentrations shown in Fig. 11 can also give us a good understanding of the effect of dopant concentration. We also notice that the difference between optimum dopant concentration according to various pump power is negligible and it is advisable to choose the suitable pump power.

In conclusion, we investigate the output properties of 976-nm fiber amplifiers considering the influence of three key factors: active fiber length, pump power, and dopant concentration. Numerical results show that the output signal power experiences a stable growth and then decreases sharply as the active fiber length becomes longer. Strong pump power which is needed to satisfy the inversion condition will not be fully utilized if the active fiber length is too short. The ASE power around 1 030 nm which limits the amplification of the signal power increases in two periods with the length of the active fiber. It is also found that the dopant concentration shows similar effects as active fiber length on the output signal power of fiber amplifiers. The results have important meanings in analyzing fiber amplifiers and will contribute to the study of high-powered MOPA fiber laser as well. In the simulation, the most optimistic pump efficiency, which is of great significant for high power fiber laser, is relatively low due to the low ratio of the core area and the inner cladding area. Further analyze will take the core/cladding area ratio and the initial signal power into consideration.

References

1. H.Injeyan and G.D.Goodno, *High-Power Laser Handbook* (The McGraw-Hill Companies, New York, 2011) pp. 518∼526.
2. H. M. Pask, P. J. Carman, D. C. Hanna, A. C. Tropper, C. J. Mackechnie, P. R. Barber, and J. M. Dawes, IEEE J. Sel. Top. Quantum Electron. **1,** 2 (1995).
3. J. Nilsson, J. D. Minelly, R. Paschotta, A. C. Tropper, and D. C. Hanna, Opt. Lett. **23,** 355 (1998).
4. A. Kurkov, O. I. Medvedkov, V. M. Paramonov, S. A. Vasiliev, E. M. Dianov, and V. Solodovnikov, in *Proceedings of Optical Amplifier and Their Applications* **OWC,** OWC2 (2001).
5. K. H. Ylä-Jarkko, R. Selvas, D. B. S. Soh, J. K. Sahu, C. A. Codemard, J. Nilsson, S. A. Alam, and A. B. Grudinin, in *Proceedings of Advanced Solid-State Photonics* **PD,** 103 (2003).
6. D. B. S. Soh, C. Codemard, J. K. Sahu, J. Nilsson, V. Philippov, C. Alegria, and Y. Jeong, in *Proceedings of Advanced Solid-State Photonics* **MA,** MA3 (2004).
7. F. Roser, C. Jauregui, J. Limpert, and A. Tünnermann, Opt. Express **16,** 17310 (2008).
8. J. Boullet, Y. Zaouter, R. Desmarchelier, M. Cazaux, F. Salin, J. Saby, R. Bello-Doua, and E. Cormier, Opt. Express **16,** 17891 (2008).
9. C. Bartolacci, M. Laroche, H. Gilles, S. Girard, T. Robin, and B. Cadier, in *Proceedings of Advanced Solid-State Photonics* **ATuB,** ATuB9 (2011).
10. A. Hardy and R. Oron, IEEE J. Quantum Electron. **33,** 307 (1997).
11. C. H. Henry, J. Lightwave Technol. **4,** 288 (1986).